LIMNOLOGY and OCEANOGRAPHY

ASLO

Limnol. Oceanogr. 66, 2021, 1961–1978

doi: 10.1002/lno.11737

Heterotrophic nitrogen fixation in response to nitrate loading and sediment organic matter in an emerging coastal deltaic floodplain within the Mississippi River Delta plain

Song Li ,[1*] **Robert R. Twilley**,[1,2] **Aixin Hou**[3]

[1]Department of Oceanography and Coastal Sciences, College of the Coast and Environment, Louisiana State University, Baton Rouge, Louisiana

[2]Louisiana Sea Grant, Louisiana State University, Baton Rouge, Louisiana

[3]Department of Environmental Sciences, College of the Coast and Environment, Louisiana State University, Baton Rouge, Louisiana

Abstract

Increasing nitrate (NO_3^-) loading in rivers due to agricultural fertilization alters benthic nitrogen (N) cycling and shifts coastal wetlands from being a net source to net sink of reactive N. Heterotrophic N_2 fixation that converts N_2 to reactive N is often assumed negligible in eutrophic ecosystems and excluded in coastal N budget evaluations. We investigated N_2 fixation and denitrification in response to increasing NO_3^- loading (0, 10, and 100 μM) and sediment organic matter ($OM_{sediment}$) concentrations in the emerging Wax Lake Delta. Continuous flow-through incubations with $^{30}N_2$ addition was applied to measure N_2 fixation. The variation of N_2 fixation rates from 0 to 437 μmol N m^{-2} h^{-1} among different NO_3^- and $OM_{sediment}$ concentrations were comparable to the estimated denitrification rates of 141–377 μmol N m^{-2} h^{-1}. Increasing overlying NO_3^- concentrations reduced N_2 fixation rates and facilitated denitrification rates at each $OM_{sediment}$ concentration. However, 100 μM of overlying NO_3^- did not thoroughly inhibit N_2 fixation rates in sites with intermediate and higher $OM_{sediment}$ concentrations (189 and 99 μmol N m^{-2} h^{-1}, respectively). Both N_2 fixation and denitrification increased with increasing $OM_{sediment}$ concentrations, but the relative importance of these processes was impacted mostly by overlying NO_3^- concentration as increasing NO_3^- switched the dominance of N_2 fixation to denitrification in benthic N cycling. This study highlights the importance of heterotrophic N_2 fixation in coastal deltaic floodplains and emphasizes the necessity of including N_2 fixation quantification in coastal N budget evaluation, not only in oligotrophic environment but also in eutrophic environment.

Agricultural fertilization has dramatically increased nitrogen (N) loading into riverine, estuarine, and coastal ecosystems, which significantly alters benthic N dynamics in response to the change of nitrate (NO_3^-) availability (Canfield et al. 2010; Koop-Jakobsen and Giblin 2010). Historical NO_3^- concentration was about 10 μM in 1900s in the Mississippi River Basin, which was 5–10 times lower than current NO_3^- concentrations ranging from 54 to 106 μM (Goolsby et al. 2000; Rabalais et al. 2002). Before humans developed industrial processes to convert N_2 gas to reactive N for agricultural use, biological N_2 fixation (both autotrophic and heterotrophic) was the key process providing reactive N while denitrification was approximately balanced with N_2 fixation (Delwiche 1970; Galloway et al. 1995; Vitousek et al. 1997). With anthropogenic increase in reactive N input to aquatic ecosystems, the energetically expensive process of heterotrophic N_2 fixation was often assumed negligible in eutrophic ecosystems (Howarth et al. 1988; Herbert 1999; Capone et al. 2008). However, recent studies indicate that heterotrophic N_2 fixation could be an important source of reactive N in many coastal and marine ecosystems using newly developed research methods of stable isotope incubations and the direct measurement of N_2 fluxes (Gardner et al. 2006; Newell et al. 2016*a*). Some observations suggest that increasing N loading can switch coastal marine sediments from being a net sink to being a net source of N_2 gas, and the dominance of denitrification rather than N_2 fixation reduces eutrophication of the coastal ocean (Fulweiler et al. 2007).

Heterotrophic N_2 fixation is performed by diazotrophic bacteria that break down the triple bond in N_2 and fix N into ammonia using the nitrogenase enzyme in concert with other cofactors and enzymes (Postgate 1970; Klotz and Stein 2008). The nitrogenase is a complex enzyme comprising a heterotetrameric

*Correspondence: sli10@lsu.edu

Additional Supporting Information may be found in the online version of this article.

core and a dinitrogenase reductase subunit that is encoded by *nifH*. A variety of *nifH* sequences exist in estuarine and coastal sediments, which makes *nifH* an ideal gene for molecular analyses of heterotrophic N-fixing microorganisms (Zehr et al. 2003; Damashek and Francis 2018). Though quantification of *nifH* gene does not necessarily mirror N_2 fixation rates, it determines the microbial potential activity for heterotrophic N_2 fixation in wetland sediments (Dias et al. 2012; Hoffman et al. 2019). Heterotrophic N_2 fixation rates and diazotrophic community composition are related to the availability of dissolved inorganic N (DIN = $NH_4^+ + NO_3^- + NO_2^-$) and organic carbon (Fulweiler et al. 2007; Scott et al. 2008; Dias et al. 2012). Heterotrophic N_2 fixation can be significantly repressed when NH_4^+ concentration is higher than 1 mM in the rhizosphere sediments of seagrass (Welsh et al. 1997; Welsh 2000) or when NO_3^- concentration is higher than 10 μM in the ocean (Mulholland et al. 2001). However, the repression is not universal as many heterotrophic diazotrophic bacteria are not sensitive to increasing concentrations of DIN (Knapp 2012; McCarthy et al. 2016). Organic matter has no consistent influence on N_2 fixation as some research indicate that heterotrophic N_2 fixation rate is higher in organic-enriched sediments (Howarth et al. 1988; McCarthy et al. 2016) while some other studies show that N_2 fixation is regulated by a complicated interplay between organic matter quality and quantity (Fulweiler et al. 2007, 2013).

Recent studies highlight the significance of heterotrophic N_2 fixation in different estuarine and coastal ecosystems with rates varying from 0 to 650 μmol N m^{-2} h^{-1} (Gardner et al. 2006; Fulweiler et al. 2007; McCarthy et al. 2016). However, fewer studies have documented the potential role of N_2 fixation in coastal deltaic floodplains at the interface of land and oceans, including mechanisms controlling N_2 fixation and the abundance of the diazotrophic community. Coastal deltaic floodplains form at the mouth of major river basins where NO_3^- removal occurs before riverine nutrients export to the ocean (Bevington and Twilley 2018; Twilley et al. 2019). Recent research at Wax Lake Delta (the delta) demonstrates that benthic NO_3^- uptake and net denitrification rates increased with greater sediment organic matter ($OM_{sediment}$) concentrations as a function of biotic feedback associated with coastal deltaic floodplain development (Li et al. 2020). Heterotrophic N_2 fixation rates may vary along the gradient of $OM_{sediment}$ concentrations, interfering the trend of denitrification rates estimated from net N_2 fluxes in response to $OM_{sediment}$ increase. Quantifying N_2 fixation rates at different $OM_{sediment}$ concentrations as a function of biotic feedback associated with deltaic succession is necessary to better understand the variation of benthic N cycles under different stages of delta development. Also, the evaluation of N_2 fixation is critical to know how much of the removed N in deltaic floodplains is associated with upstream N enrichment.

There is evidence that the dominant N pathway has switched from N_2 fixation to denitrification in the delta in response to an increase of riverine NO_3^- (from 2 to > 60 μM) that shifts net N_2 fluxes from negative (uptake from water column to sediment) to positive (release from sediment to water column; Henry and Twilley 2014). This change of the net N_2 fluxes could be because the increased NO_3^- concentrations either inhibited N_2 fixation or facilitated both processes but favored denitrification more than N_2 fixation. If it is the first situation, it is uncertain whether N_2 fixation is totally suppressed or partially inhibited at higher overlying NO_3^- concentration. Investigating N_2 fixation and the relative contribution of N_2 fixation and denitrification to net N_2 fluxes under the impacts of increasing NO_3^- concentrations are necessary to clarify the role of coastal deltaic floodplains in benthic N cycling in response to decadal changes in river fertilization.

We studied Wax Lake Delta, a young (47 yr) coastal deltaic floodplain, to investigate the response of N_2 fixation and denitrification to increased NO_3^- loading and $OM_{sediment}$ concentrations. The delta receives a large amount of riverine NO_3^- (3300–8600 mg of N) per yr as 23–54% of eutrophic riverine water discharge from primary channels enters the interdistributary islands of the delta (Lane et al. 2002; Hiatt and Passalacqua 2015; Li et al. 2020). The coastal deltaic floodplain in this large delta estuary removes 10–27% of riverine NO_3^- through denitrification prior to export to the ocean (Li et al. 2020; Li and Twilley, 2021). The patterns of benthic nutrient fluxes and pathways of N cycling vary in response to an increasing $OM_{sediment}$ concentrations resulting from morphological development with delta age, which makes the delta an ideal system to study the significance of N_2 fixation under different $OM_{sediment}$ and nutrient loading conditions (Li et al. 2020; Li and Twilley, 2021). Denitrification rates have already been measured directly with $^{15}NO_3^-$ enrichment using isotope pairing technique along a gradient of $OM_{sediment}$ concentrations in the delta (Li and Twilley, 2021), and this research focuses on the variation of N_2 fixation during the development of coastal deltaic floodplain. This research continues to develop an understanding of how ecological feedback on geomorphology development of deltaic floodplains alters the N cycles of these newly emergent ecosystems (Twilley et al. 2019).

In this research, incubations of intact sediment cores with $^{30}N_2$ tracer were conducted to measure heterotrophic N_2 fixation directly. The abundance of *nifH* gene and $\delta^{15}N$ of the total N in incubated sediments were measured to support the occurrence of N_2 fixation. Simultaneous measurements of denitrification and N_2 fixation are difficult because denitrification releases N_2 gas whereas N_2 fixation consumes N_2 gas. Here, we used estimated denitrification rates from Redfield stochiometric ratios based on Li et al. 2020 and we compared these estimated denitrification rates with N_2 fixation rates. We evaluated benthic N budgets with a major focus on N_2 fixation and denitrification under different NO_3^- concentrations at the relatively earlier and later successional stages in the delta. Specific research questions addressed include the following. (1) How will increasing NO_3^- concentrations in overlying water impact heterotrophic N_2 fixation rates under different

$OM_{sediment}$ concentrations? (2) How does the relative importance of N_2 fixation and denitrification change with the increasing NO_3^- loading and $OM_{sediment}$ concentrations?

Methods

Wax Lake Delta forms at the mouth of the Wax Lake outlet in coastal Louisiana within the Atchafalaya Basin in the Mississippi River Delta (Fig. 1). The delta is river-dominated with the land growth rate of 2.62 km^2 per yr (Edmonds et al. 2011; Paola et al. 2011; Twilley et al. 2019). The delta is primarily composed of mineral sediments with an increasing gradient of $OM_{sediment}$ associated with morphological development along the chronosequence from younger to older deltaic area (Bevington and Twilley 2018; Li et al. 2020). The delta provides a natural lab of deltaic processes to investigate the relative important of N_2 fixation and denitrification in response to increasing NO_3^- loading and $OM_{sediment}$ concentrations.

Field sampling and experiments were conducted at three experimental sites representing lower sediment organic matter (lower-$OM_{sediment}$), intermediate sediment organic matter (int-$OM_{sediment}$) and higher sediment organic matter (higher-$OM_{sediment}$; Fig. 1). The lower-$OM_{sediment}$ site is a younger subtidal hydrogeomorphic site with mainly mineral sedimentation at the earlier successional stage of delta development. The int- and higher-$OM_{sediment}$ sites at the later successional stage of delta development are older experimental sites located more near delta apex with higher soil elevation and $OM_{sediment}$ concentrations. The int-$OM_{sediment}$ site is located near the fringe along a primary channel of the delta and exposed to frequent flood pulses of inorganic sedimentation, thus its $OM_{sediment}$ concentration is relatively lower than the higher-$OM_{sediment}$ site located within the interior of the island. Detailed descriptions of these experimental sites are shown in Li and Twilley (2021). The int-, higher-, and lower-$OM_{sediment}$ sites were sampled on 22 June, 06 July, and 20 July, respectively, in 2019. Unfortunately, 1 week before the field sampling of the lower-$OM_{sediment}$ site a hurricane (Barry) occurred 70 km to the west of the delta. Though the hurricane might interfere with benthic activity in the lower-$OM_{sediment}$

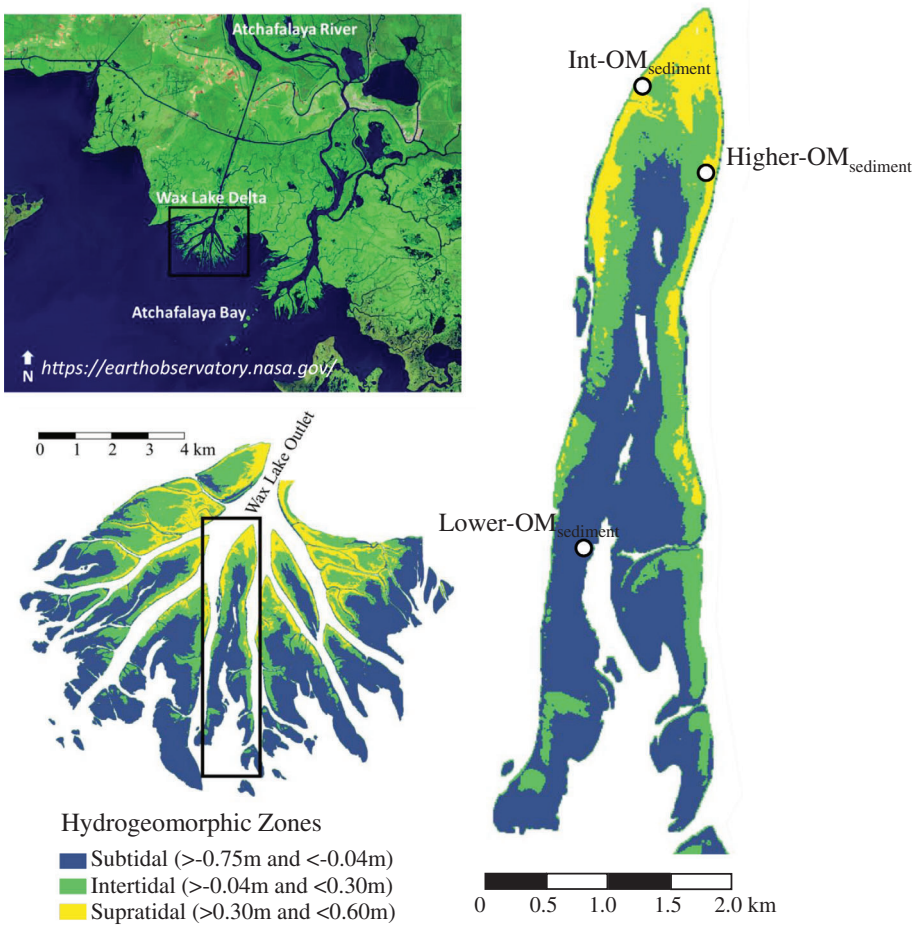

Fig 1. Location of sampling sites across Mike Island in the Wax Lake Delta, Louisiana, at the lower (lower-$OM_{sediment}$), intermediate (int-$OM_{sediment}$), and higher (higher-$OM_{sediment}$) sediment organic matter concentrations. Elevation records are based on USGS Atchafalaya 2 project LiDAR Survey 2012 digital elevation model (4-m horizontal resolution and 0.01-m vertical resolution, Bevington and Twilley, 2018).

site, we still collected samples and incubated cores the same way as we treated the other two sites. We compared the post-hurricane sediment property and benthic fluxes in the lower-$OM_{sediment}$ site to the corresponding results measured in the same site in summer 2018 (Li and Twilley, 2021) to evaluate the possible hurricane effects to benthic N dynamics.

Duplicate surface water (right below the air–water interface) and pore water (4 cm below the sediment–water interface using rigid aquarium tubing affixed to a 60-mL syringe) samples were collected and filtered (GF/F glass microfiber filters, 0.7 μm particle retention) in each of the three experimental sites for the analysis of inorganic nutrients. Concentrations of NO_3^-, nitrite (NO_2^-), ammonium (NH_4^+), and phosphate (PO_4^{3-}) were analyzed on a segmented flow solution IV autoanalyzer (OI analytical, College Station, Texas). Triplicate ambient samples of the top 4 cm sediments were sampled in each site in the field using a piston core (2.4 cm internal diameter), then oven dried at 60°C to constant mass and ground to <250 μm for the isotope ratio analysis of total ^{15}N in sediments using an isotope ratio mass spectrometer (Sercon 20/20 ANCA-GLS). In situ water temperature, salinity, and dissolved O_2 concentrations were measured using a portable YSI salinity–conductivity–temperature meter (model 30, YSI Incorporated, Yellow Springs, Ohio) and a dissolved oxygen meter (HQ40d, Hach, Loveland, Colorado).

Nine intact sediment cores (about 10 cm internal diameter) with 10 ± 1 cm depth of sediments and 10 ± 1 cm of overlying water were collected from each experimental site and sealed with silicone-greased bottoms and detachable lids. Cores were then stored in a cooler at in situ temperature and transported to the lab within 4 h. In the lab, the nine sediment cores from each site were randomly assigned to three treatments of NO_3^-concentrations at 0, 10, and 100 μM in incubation solutions. The incubation solutions were riverine waters collected from Wax Lake outlet and filtered using a five-stage filtration system (30, 20, 5, 1, and 0.2 μm) several days before the sampling date. These filtered waters flowed through packed column of NO_3^--specific resin (ResinTech SIR-100-HP, West Berlin, New Jersey) to remove all background NO_3^-, then stored in 25-liter gas-tight Tedlar bags (Keika Ventures) at 4°C until incubations. Three Tedlar bags of water were brought to room temperature and injected with 120 mL of $^{30}N_2$ gas (98%, Cambridge Isotope Laboratories) per Tedlar bag at room temperature and atmospheric pressure 24 h before every incubation event. All bags with water and injected $^{30}N_2$ gas were shaken gently for 5 min every 3–4 h until the beginning of an incubation event. Extra gas bubbles in Tedlar bags were gently squeezed out and different amounts of KNO_3 (^{14}N) were added to the three bags to make water NO_3^-concentrations at 0, 10, and 100 μM, respectively, right before the incubations (Fig. 2). An extra bag of water was prepared with the similar amount of $^{30}N_2$ injection under the same condition to incubate two blank cores with only 10 cm of treated water during every incubation event. The incubations of blank cores were used to correct all possible gas diffusion and interferences not related to benthic activities. There are three incubation events in total (each one focused on one experimental site) and one of the three NO_3^-concentrations (0, 10, and 100 μM) were assigned to the blank core incubation in each incubation event to correct the possible change in NO_3^-concentrations not related to benthic activities.

The ambient overlying water in blank and sediment cores were gently replaced with treatment solutions and installed into a continuous flow-through system in a dark chamber at room temperature (Miller-Way and Twilley 1996; Li et al. 2020). We adjusted the flow rate of influent solutions to establish a residence time of about 3 h for the overlying water in each core. A 10-h preincubation period was conducted to allow fluxes at sediment–water interfaces to approach an equilibrium. Following the preincubation period, influent and effluent solutions were sampled at 3-h interval of the residence time for a total of three turnovers per experiment. We assumed sediment cores achieved steady state fluxes (no significant variance of flux with time) for each turnover of overlying water and differences between the influent and effluent concentrations of inorganic nutrients and dissolved gases were primarily due to processes at the sediment–water interface such as denitrification, N_2 fixation, and so on (Miller-Way and Twilley 1996). These assumptions were tested for each independent turnover of water in each experimental site (*see* supporting information Data S1 to show statistical tests of these assumptions).

Duplicate influent and effluent water samples were collected and filtered through 25 mm GF/F glass microfiber filters (0.7 μm particle retention) in each sampling event. Samples were frozen (−20°C) until analyzed for NH_4^+, NO_2^-, NO_3^-, and PO_4^{3-} concentrations on a flow solution IV autoanalyzer. Duplicate samples for influent and effluent dissolved gas analyses were collected into 12-mL gas-tight exetainers (Labco Limited, Lampeter, Wales, UK) with 200 μL addition of $ZnCl_2$ solution (50% saturation concentration, Nielsen and Glud 1996). Gas samples were stored underwater at 4°C until analyzed for $^{28}N_2$, $^{29}N_2$, and $^{30}N_2$ within 1 month on a membrane inlet mass spectrometer (MIMS) with a copper column heated to 600°C (Kana et al. 1994; Eyre et al. 2002). Dissolved oxygen concentrations of influent and effluent waters were measured using a Hach HQ30L DO probe at the end of each water residence time.

Benthic fluxes of dissolved gas and inorganic nutrients were calculated using the equation:

$$\text{Flux} = \frac{[(C_e - C_i) - (C_{be} - C_{bi})] \times \text{flow rate}}{\text{Core surface area}}, \quad (1)$$

where C_e and C_i are effluent and influent concentrations (μM) of a sediment core whereas C_{be} and C_{bi} are averaged effluent and influent concentrations of blank cores in the corresponding incubation event. Denitrification rates were estimated based on a stochiometric assumption that the molar oxygen (O) : N ratios of sediment fluxes follow the Redfield composition (O : N = 138 : 16).

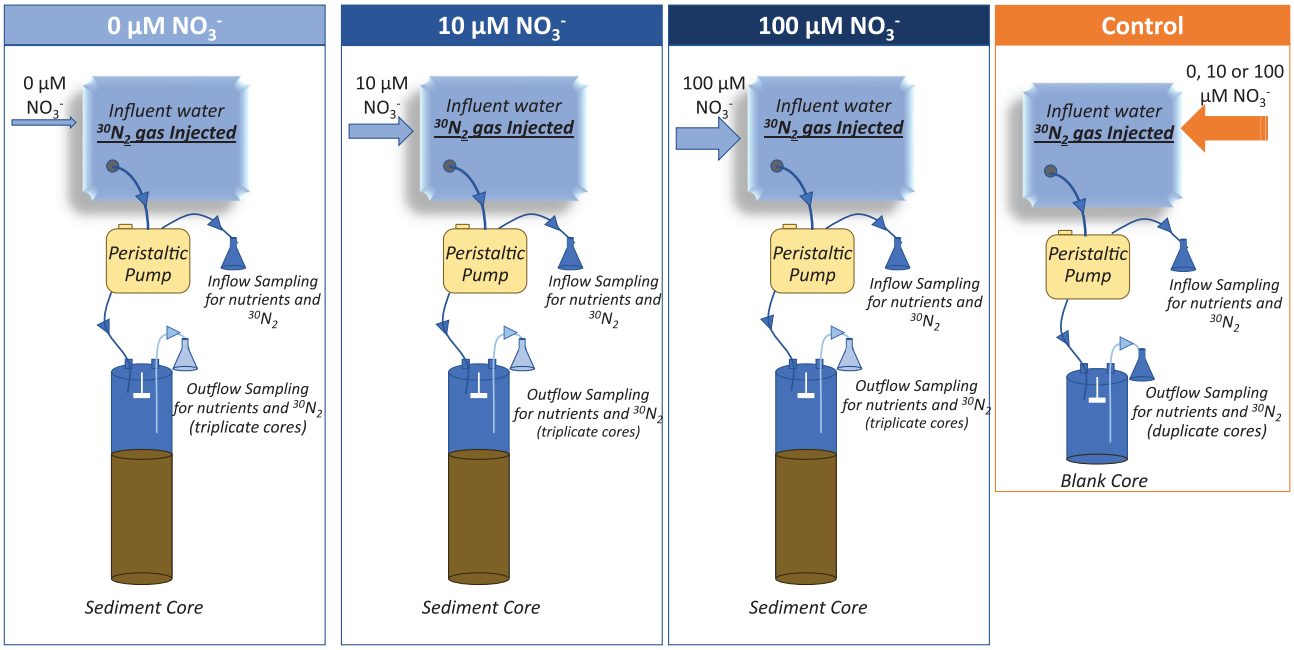

Fig 2. Diagram of experimental setup using continuous flow-through incubations across three treatments and controls. Triplicate cores were used in each treatment and duplicated cores were used in each control.

Denitrification rates refer to the discrepancy between the measured fluxes of DIN ($NH_4^+ + NO_3^- + NO_2^-$) and the estimated fluxes of DIN based on benthic oxygen consumptions multiplied by the Redfield ratio of 16/138 (Cowan et al. 1996; Cornwell et al. 1999; Li et al. 2020).

We used the estimated rates of denitrification because recent research demonstrated that denitrification rates calculated from stochiometric method are ideal estimates of denitrification rates in our study area (Supporting Information Fig. S1, Li et al. 2020). To support this assumption, we compared the estimated denitrification rates with recent measured denitrification rates in the same experimental sites under similar incubation conditions (Li and Twilley, 2021). We verified that the estimated denitrification rates were in the same magnitude as the measured denitrification rates using isotope pairing technique in each experimental site. We compared the estimated denitrification rates with net N_2 fluxes ($^{28}N_2$, $^{29}N_2$, and $^{30}N_2$) and calculated N_2 fixation rates only when estimated denitrification rates were greater than net N_2 effluxes (from sediments to overlying water column). Heterotrophic N_2 fixation rates were calculated from the estimated denitrification rates minus net N_2 effluxes.

After the incubations, duplicate samples of the top 4-cm sediments in each sediment core were collected using a piston core (2.4-cm internal diameter). One set of sediment samples (totally 27 samples from three experimental sites) was frozen for DNA extraction and quantitative polymerase chain reaction (qPCR) analysis. The other set of sediments was oven-dried at 60°C to constant mass to determine bulk density (g cm^{-3}) using dry sediment mass divided by wet sediment volume (8.75 cm^3). We determined $OM_{sediment}$ concentrations (% dry mass) by grinding each dried sediment sample to <250 μm, weighting out 1 ± 0.01 g subsample and igniting at 550°C for 2 h. Certain amounts (based on instrument limitation) of the dried and powdered sediment samples were weighed into tin capsules and analyzed together with the ambient sediment samples collected in the field on the isotope ratio mass spectrometer for $\delta^{15}N_{Air}$ of total N (‰, the deviation of the $^{15}N/^{14}N$ ratio in a sample from the corresponding isotope ratio in the reference material of air-N_2).

Sediment samples for DNA extraction were ground in liquid N_2 and preserved at −80°C. The use of liquid N_2 during grinding process preserved the samples in freezing and effectively prevented the degradation of DNA and RNA (de Felippes and Weigel 2010). DNA and RNA were extracted from 2 ± 0.01 g sediment per sample using the RNeasy PowerSoil total RNA kit and RNeasy PowerSoil DNA elution kit (Qiagen). Quality and quantity of the DNA and RNA extracts were checked spectrophotometrically (nanodrop ND-2000C, Thermo Scientific). RNA was found degraded due to mis-preservation, and thus, we only quantified the key functional gene of *nifH* in DNA. We used the PolF (TGC GAY CCS AAR GCB GAC TC) and PolR (ATS GCC ATC ATY TCR CCG GA) primers to amplify the 361-bp *nifH* fragment (Poly et al. 2001). A standard curve of qPCR was made by amplifying *nifH* gene using conventional PCR technique, followed by purification, cloning and serial plasmid dilutions of the PCR product extracted from agarose gel (Fan 2013). We used a 20-μL reaction mixture including 2-μL template DNA (about 10–40 ng μL^{-1} after 10 times dilution), 1 μL of each primer

(10 μM), 6-μL real time-qPCR grade water, and 10-μL PowerUp SYBR green master mix. Quantitative real-time PCR was performed on a CFX Connect Real-time system (Bio-RAD) with the thermocycling conditions including 5 min at 95°C, 35 cycles of 30 s at 95°C, 30 s at 55°C, and 40 s at 72°C. A melting curve analysis was done after the amplification by heating the products from 50°C to 95°C at a rate of 0.5°C s^{-1}, the results of which confirmed the specificity of the amplification. All qPCR analyses were performed in two 96-well plates with each of the seven standards in triplicate, samples in triplicates, a no-template control in each plate, and several repeated samples between plates to check the consistency between two assays. The efficiencies for standard curves ranged from 97% to 101% and the R^2 values were over 0.99. The gene copy numbers were calculated based on nanograms of amplicon following the equation:

$$\text{Gene copy number} = \frac{\text{Amount (ng)} \times \text{Abundance}\left(6.022 \times 10^{23}\,\text{mol}^{-1}\right)}{\text{bp (361)} \times \text{ng g}^{-1}\left(10^{9}\right) \times \text{g mol}^{-1}\text{of bp (660)}}. \quad (2)$$

One-way ANOVA was used to test the significance of $OM_{sediment}$ and bulk density among the experimental sites. The significance of inorganic nutrient, dissolved gas fluxes as well as N_2 fixation and denitrification rates among the treatments and experimental sites were tested using repeated measures ANOVAs with three sampling events in each core as the repeated measures. Benthic fluxes did not show significant difference among the three sampling time series (3, 6, and 9 h after preincubation, *see* supporting information Table S1), indicating that incubations in each site achieved steady state during the sampling period. Two-way ANOVA was used to test the difference of *nifH* copy numbers per gram of dry sediment in response to the interaction between study sites and NO_3^- treatments. We did Shapiro–Wilk normality tests before ANOVA tests and used Box–Cox transformations and some other transformations (JMP software) to achieve normality for some sets of data that were not normally distributed before ANOVA tests (Supporting Information Table S2). Tukey's HSD post hoc test with all pairwise comparisons was used when differences were significant at a 95% confidence level. The difference of the $\delta^{15}N_{Air}$ values of total N between the ambient sediments and incubated sediments under different treatments in every experimental site was tested using ANOVA followed by Dunnett's test at $p < 0.05$. Data analyses were conducted using JMP software and results were presented as means with error bars of standard error (SE).

Results

Characteristics of experimental sites and lab incubations

There was a strong decrease in sediment bulk density from 1.2 to 0.2 g cm^{-3} and increase in $OM_{sediment}$ concentrations from 4.5% to 20.6% from the lower-$OM_{sediment}$ site (younger subtidal area) to higher-$OM_{sediment}$ site (older supratidal area, Fig. 3). The study area is a tidal freshwater wetland with salinity ≤ 0.2 in surface waters and 0.2–0.5 in pore waters (Table 1). NO_3^- concentrations of in-situ surface water ranged from 58.0 μM at the lower-$OM_{sediment}$ site to 6.6 μM at the higher-$OM_{sediment}$ site, which were higher than NO_3^- concentrations in pore water in the corresponding site. NH_4^+ concentrations were low in the in-situ surface water (0.5–5.4 μM) but high in the pore water (41.3–182.6 μM). NO_2^- and PO_4^{3-} concentrations of the in situ surface water and pore water were low in all the experimental sites. Lab incubations were conducted in a water bath controlling the temperature at 19.5–21.9°C with influent water saturated with dissolved oxygen (Table 2). All sediment cores were incubated under similar physical and chemical conditions except for the three different treatments of influent NO_3^- concentrations.

Sediment oxygen consumption and benthic nutrient fluxes

Mean rates of sediment oxygen consumption were not significantly different among the three NO_3^- treatments for each

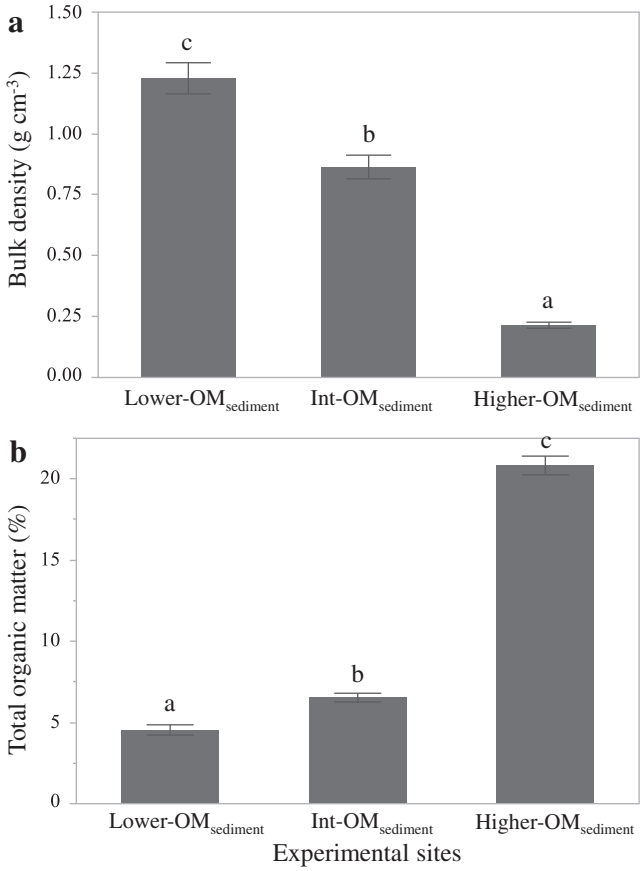

Fig 3. (**a**) Bulk density and (**b**) organic matter concentrations in the top 4 cm of sediment in the three experimental sites representing lower (lower-$OM_{sediment}$), intermediate (int-$OM_{sediment}$) and higher (higher-$OM_{sediment}$) sediment organic matter concentrations (mean ± 1 SE, $n = 9$). Letters designate significant differences among experimental sites using Tukey's HSD test ($p < 0.05$).

Table 1. Ambient surface water and pore water conditions in experimental sites including lower (lower-$OM_{sediment}$), intermediate (int-$OM_{sediment}$), and higher (higher-$OM_{sediment}$) sediment organic matter in Wax Lake Delta, Louisiana. There was no measurement of dissolved O_2 concentration in pore-water samples.

	Surface water			Porewater		
	Lower-$OM_{sediment}$	Int-$OM_{sediment}$	Higher-$OM_{sediment}$	Lower-$OM_{sediment}$	Int-$OM_{sediment}$	Higher-$OM_{sediment}$
Salinity	0.2	0.2	0.2	0.5	0.3	0.2
O_2 (mg L^{-1})	4.6	5.2	2.1	NA	NA	NA
NO_3^- (μM)	58.0	56.7	6.6	1.4	5.5	0.1
NO_2^- (μM)	0.9	0.3	2.1	0.3	0.8	0.1
NH_4^+ (μM)	0.5	2.3	5.4	182.6	41.3	97.7
PO_4^{3-} (μM)	2.7	2.2	1.6	0.4	0.7	1.4

Table 2. Incubation conditions of intact sediment cores at different overlying NO_3^- concentrations in each of the three experimental sites representing lower (lower-$OM_{sediment}$), intermediate (int-$OM_{sediment}$), and higher (higher-$OM_{sediment}$) sediment organic matter concentrations in Wax Lake Delta, Louisiana. The three treatments of overlying NO_3^- concentrations were: 0 μM NO_3^- enrichment, 10 μM NO_3^- enrichment and 100 μM NO_3^- enrichment.

	Lower-$OM_{sediment}$			Int-$OM_{sediment}$			Higher-$OM_{sediment}$		
	0 μM NO_3	10 μM NO_3	100 μM NO_3	0 μM NO_3	10 μM NO_3	100 μM NO_3	0 μM NO_3	10 μM NO_3	100 μM NO_3
Temp (°C)	19.5	19.5	19.5	21.9	21.9	21.8	21.5	21.6	21.6
O_2 (mg L^{-1})	9.7	9.5	9.4	8.3	8.1	8.3	9.4	9.4	9.5
NO_3 (μM)	0.0	9.1	85.9	0.4	9.9	86.0	1.4	10.5	86.2
NO_2 (μM)	0.1	0.1	0.0	0.0	0.0	0.0	0.1	0.1	0.1
NH_4 (μM)	0.9	0.9	1.0	1.0	0.9	1.4	1.8	1.6	2.1
PO_4 (μM)	0.2	0.2	1.2	0.8	0.8	0.6	1.4	0.7	0.6

site, but there was a significant increase ($p < 0.0001$) from lower to higher $OM_{sediment}$ sites for each NO_3^- concentration (Table 3). Benthic NO_3^- fluxes were significantly different among both the three NO_3^- treatments ($p < 0.0001$) and sites ($p = 0.005$). Benthic NO_3^- uptakes increased from 21.7 ± 2.4 to -157.6 ± 44.8 μmol m^{-2} h^{-1} in the lower-$OM_{sediment}$ site with increasing NO_3^- loading from 0 to 100 μM. Similarly, benthic NO_3^- uptakes increased from 10.0 ± 3.7 to -260.0 ± 52.1 μmol m^{-2} h^{-1} in the int-$OM_{sediment}$ site and from -13.5 ± 4.3 to -213.9 ± 35.5 μmol m^{-2} h^{-1} in the higher-$OM_{sediment}$ site as overlying NO_3^- loading increased from 0 to 100 μM. NO_3^- fluxes in the int- and higher-$OM_{sediment}$ sites were more negative (uptake from water columns to sediments) than fluxes in the lower-$OM_{sediment}$ site in each of the three NO_3^- treatments. NH_4^+ fluxes were positive (release from sediments to water columns) with an increase in NO_3^- concentrations from 0 to 100 μM in each of the experimental sites. The higher-$OM_{sediment}$ site was significantly higher in benthic NH_4^+ release (67.3 ± 11.61 μmol m^{-2} h^{-1}, $p = 0.03$) than the other two sites (27.1 ± 4.0–33.1 ± 10.3 μmol m^{-2} h^{-1} in int-and lower-$OM_{sediment}$ site, respectively) in each NO_3^- treatment. NO_2^- fluxes in 0 and 10 μM treatments (1.3 ± 0.3–1.6 ± 0.2 μmol m^{-2} h^{-1}, respectively) were significantly lower ($p < 0.0001$) than the fluxes of 11.0 ± 1.7 μmol m^{-2} h^{-1} in 100 μM NO_3^- treatment. There was no clear trend of NO_2^- fluxes among the $OM_{sediment}$ gradient. The benthic fluxes of PO_4^{3-} did not show clear patterns among the treatments or experimental sites.

Nitrogen fluxes in response to N_2 fixation and denitrification

$^{30}N_2$ fluxes were mostly negative under different NO_3^- treatments in the three experimental sites, indicating the occurrence of N_2 fixation that consumed $^{30}N_2$. The int-$OM_{sediment}$ site showed significantly higher $^{30}N_2$ uptake ($p < 0.0001$), especially at 0 and 10 μM NO_3^- treatments (Fig. 4a). In contrast, the lower-$OM_{sediment}$ site had significantly lower $^{30}N_2$ uptake ($p < 0.0001$) regardless of the overlying NO_3^- concentrations. Net fluxes of the sum of $^{28}N_2$, $^{29}N_2$, and $^{30}N_2$ were mostly positive under different treatments in the three experimental sites (Fig. 4b). Net fluxes of the sum of $^{28}N_2$, $^{29}N_2$, and $^{30}N_2$ indicated a combined signal of

Table 3. Benthic fluxes of dissolved oxygen and inorganic nutrients at different overlying NO_3^- concentrations in each of the three experimental sites representing lower (lower-$OM_{sediment}$), intermediate (int-$OM_{sediment}$), and higher (higher-$OM_{sediment}$) sediment organic matter concentrations in Wax Lake Delta, Louisiana. The three treatments of overlying NO_3^- concentrations were: 0 μM NO_3^- enrichment, 10 μM NO_3^- enrichment and 100 μM NO_3^- enrichment.

	Lower-$OM_{sediment}$			Int-$OM_{sediment}$			Higher-$OM_{sediment}$		
Flux	**0 μM NO_3**	**10 μM NO_3**	**100 μM NO_3**	**0 μM NO_3**	**10 μM NO_3**	**100 μM NO_3**	**0 μM NO_3**	**10 μM NO_3**	**100 μM NO_3**
O_2 (g O_2 m^{-2} d^{-1})	−0.3	−0.5	−0.5	−1.5	−1.6	−1.3	−1.7	−2.2	−1.9
(SE)	(0.0)	(0.0)	(0.2)	(0.1)	(0.1)	(0.1)	(0.1)	(0.1)	(0.2)
NO_3^- (μmol m^{-2} h^{-1})	21.7	7.3	−157.6	10.0	−97.2	−260.0	−13.5	−49.6	−213.9
(SE)	(2.4)	(3.3)	(44.8)	(3.7)	(25.9)	(52.1)	(4.3)	(5.4)	(35.5)
NO_2^- (μmol m^{-2} h^{-1})	1.6	1.8	4.6	1.7	1.3	14.4	0.7	1.8	14.2
(SE)	(0.4)	(0.4)	(1.6)	(0.6)	(0.5)	(3.3)	(0.2)	(0.2)	(2.5)
NH_4^+ (μmol m^{-2} h^{-1})	19.6	20.5	59.3	19.0	25.1	37.2	32.7	56.9	112.5
(SE)	(8.2)	(5.3)	(28.3)	(3.6)	(5.2)	(9.7)	(16.4)	(13.9)	(20.9)
PO_4^{3-} (μmol m^{-2} h^{-1})	1.1	−7.4	−7.1	10.1	13.7	8.4	−6.8	9.3	−1.5
(SE)	(0.5)	(0.6)	(3.1)	(1.3)	(3.5)	(1.6)	(1.7)	(3.7)	(0.5)

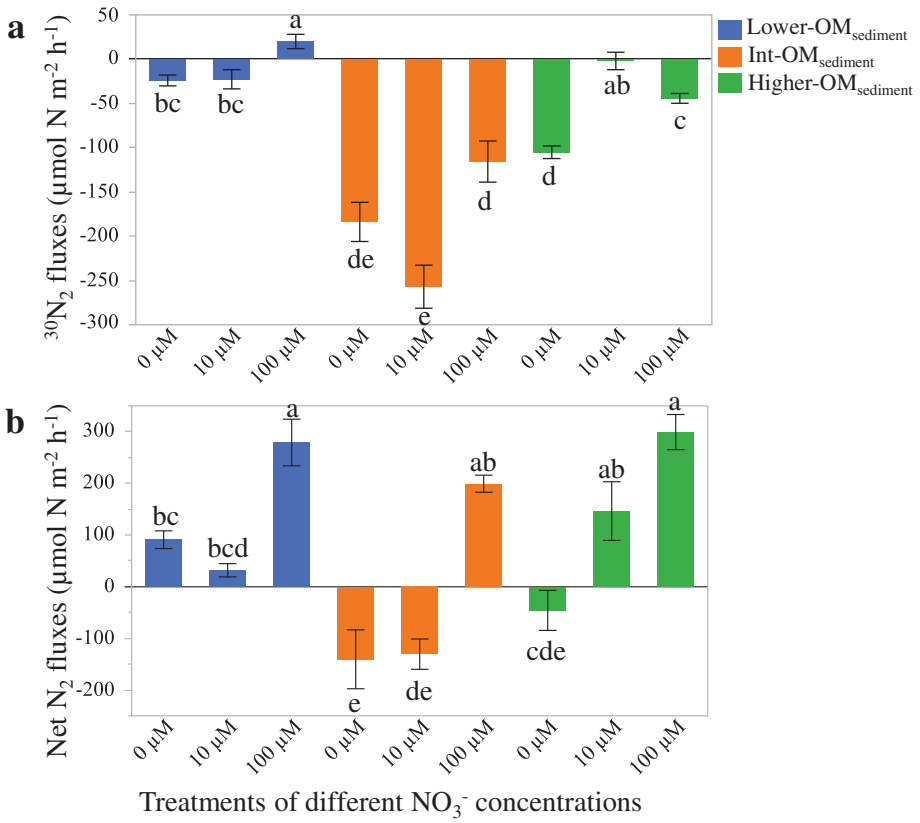

Fig 4. (**a**) Benthic fluxes of $^{30}N_2$ and (**b**) net fluxes of $^{28+29+30}N_2$ at the sediment–water interface across the three treatmeeents of NO_3^- addition in the experimental sites representing lower (lower-$OM_{sediment}$), intermediate (int-$OM_{sediment}$) and higher (higher-$OM_{sediment}$) sediment organic matter concentrations (mean ± 1 SE, $n = 9$). Letters designate significant differences among the interaction of experimental sites and treatments using Tukey's HSD test ($p < 0.05$).

denitrification and N_2 fixation as positive fluxes demonstrated a dominance of denitrification that produces N_2 whereas negative fluxes demonstrated a dominance of N_2 fixation rather than denitrification. The lower-$OM_{sediment}$ site had positive net fluxes of $^{28}N_2$, $^{29}N_2$, and $^{30}N_2$ with significantly higher fluxes in 100 μM NO_3^- treatment compared to the other two (0 and

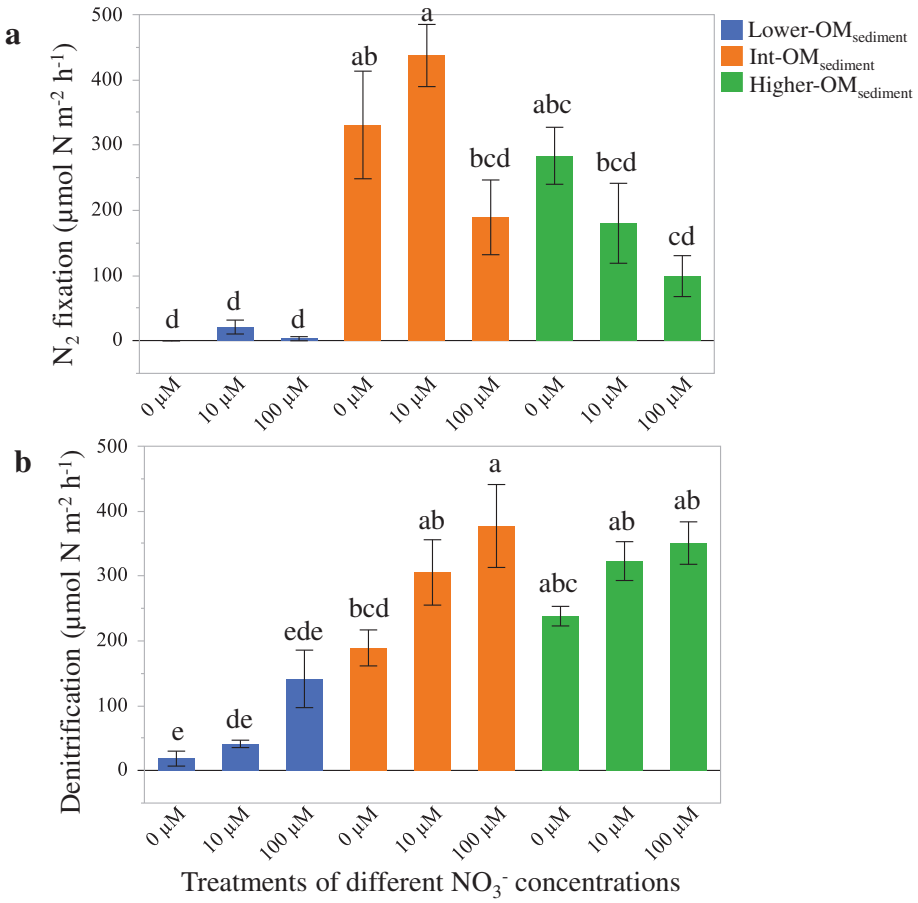

Fig 5. (**a**) Heterotrophic N_2 fixation rates determined by the sum of $^{28+29+30}N_2$ fluxes minus the estimated denitrification rates and (**b**) estimated denitrification rates from the discrepancy between the measured fluxes of DIN ($NH_4^+ + NO_3^- + NO_2^-$) and the estimated fluxes of DIN based on benthic oxygen consumptions multiplied by the Redfield ratio of 16/138 (mean ± 1 SE, $n = 9$; Li et al., 2020). Letters designate significant differences among the interaction of experimental sites and treatments using Tukey's HSD test ($p < 0.05$). Sites include lower (lower-OM$_{sediment}$), intermediate (int-OM$_{sediment}$) and higher (higher-OM$_{sediment}$) sediment organic matter concentrations.

10 μM) NO_3^- treatments (Fig. 4b). In the int-OM$_{sediment}$ site, increasing overlying NO_3^- concentrations from 0 and 10 to 100 μM shifted the negative net N_2 fluxes (−130.6 to −140.6 μmol N m^{-2} h^{-1}) to positive fluxes (199.4 μmol N m^{-2} h^{-1}). A similar pattern was observed in the higher-OM$_{sediment}$ site as net N_2 fluxes switched from negative to positive with the increasing overlying NO_3^- concentrations.

Heterotrophic N_2 fixation rates in the lower-OM$_{sediment}$ site (0–21.0 μmol N m^{-2} h^{-1}) were significantly lower ($p < 0.05$) than the other two sites regardless of overlying NO_3^- treatments (Fig. 5a). Denitrification rates in the lower-OM$_{sediment}$ site increased from 18.5 to 141.4 μmol N m^{-2} h^{-1} as overlying NO_3^- concentrations increased from 0 to 100 μM (Fig. 5b). Heterotrophic N_2 fixation rates in the int-OM$_{sediment}$ site ranged from 189.2 to 437.3 μmol N m^{-2} h^{-1} with a lower N_2 fixation rate in 100 μM NO_3^- treatment compared to the other two (0 and 10 μM) NO_3^- treatments. Denitrification rates in the int-OM$_{sediment}$ site increased significantly ($p < 0.0001$) with the increased NO_3^- concentrations from 0 to 100 μM. The range of denitrification rates from 189.1 to 377.1 μmol N m^{-2} h^{-1} in the int-OM$_{sediment}$ site were comparable with the N_2 fixation rates in this site. The higher-OM$_{sediment}$ site had a decrease in N_2 fixation rates from 283.6 to 52.6 μmol N m^{-2} h^{-1} and an increase in denitrification rates from 238.1 to 350.7 μmol N m^{-2} h^{-1} as overlying NO_3^- concentration increased from 0 to 100 μM.

We detected the presence of *nifH* gene in all three experimental sites under different NO_3^- treatments (Fig. 6). The *nifH* copy numbers per gram of dry sediment revealed significant difference ($p < 0.0001$) in diazotrophic community abundances across the three experimental sites with different OM$_{sediment}$ concentrations. $\delta^{15}N_{Air}$ values significantly increased ($p < 0.0001$) from the lower-OM$_{sediment}$ site (4.9 ‰) to the higher-OM$_{sediment}$ site (7.7 ‰) in the ambient sediment samples collected in the field (light gray columns in Fig. 7). The $\delta^{15}N_{Air}$ values after incubations were slightly higher than the respective preincubation values in the ambient sediments, especially under lower overlying NO_3^- additions (0 and 10 μM). But only the lower-OM$_{sediment}$ site at 0 μM NO_3^-

addition (p = 0.026) and the higher-$OM_{sediment}$ site at 0 and 10 μM NO_3^- additions (p = 0.0042 and 0.0051, respectively) indicated significant differences of $\delta^{15}N_{Air}$ values compared to values in the corresponding ambient sediments based on Dunnett's test (asterisked in Fig. 7).

Discussion

Nitrogen fixation affected by nitrate loading and $OM_{sediment}$ concentrations

Heterotrophic N_2 fixation rates are frequently excluded in benthic N budgets as previous indirect measurements indicated that N_2 fixation rates are not significant in coastal ecosystems (Howarth et al. 1988; Damashek and Francis 2018). However, recent research revealed that N_2 fixation is a significant part of N cycle in estuarine and coastal sediments using improved methods of isotope enrichments (either NO_3^- or $^{30}N_2$) with intact-core incubations and *nifH* quantification (An et al. 2001; Fulweiler et al. 2007; Newell et al. 2016*a*). Direct measurement of N_2 fixation that fixes N_2 to reactive N is necessary to define the role of coastal deltaic floodplains in processing eutrophic riverine water.

We evaluated sediment N_2 fixation directly with the $^{30}N_2$ tracer addition in response to increasing overlying NO_3^- concentrations in the emerging delta with different $OM_{sediment}$ concentrations representing different stages of morphological development. Lower $OM_{sediment}$ concentrations occur in younger subtidal hydrogeomorphic sites due to mineral sedimentation dominating the earlier stages of delta development while intermediate and higher $OM_{sediment}$ concentrations occur in older supratidal sites with greater biotic feedbacks associated with ecological succession (Bevington and Twilley, 2018; Li and Twilley, 2021). The occurrence of N_2 fixation in the research area was also supported by the measured *nifH* gene abundances in the three experimental sites. $\delta^{15}N_{Air}$ results showed slight increase in incubated sediments with $^{30}N_2$ enriched influent water compared to $\delta^{15}N_{Air}$ values in ambient sediments, especially when overlying NO_3^- concentrations were lower (0 and 10 μM), indicating the occurrence of N_2 fixation in the delta. The increased signal of $\delta^{15}N_{Air}$ in the top layer of sediments may be more significant if the 20-h incubation is extended to a longer duration (Newell et al. 2016*a*).

The rates of N_2 fixation from 0 to 437 μmol N m^{-2} h^{-1} measured in this study were comparable to heterotrophic N_2 fixation rates of 0–650 μmol N m^{-2} h^{-1} reported in other estuarine and coastal ecosystems (Table 4). Our study area had slightly higher *NifH* gene abundance than *nifH* copies reported in saline ecosystems. The possible reason is that Wax Lake

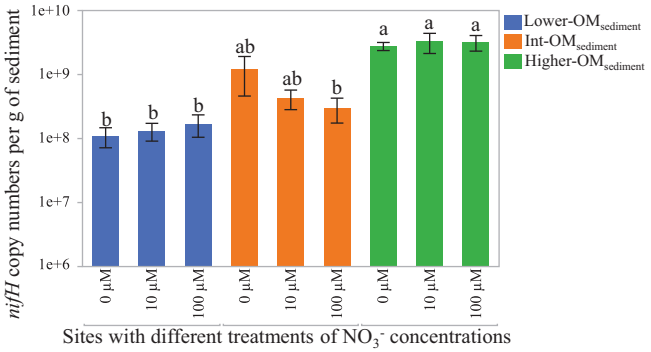

Fig 6. *NifH* copy numbers in DNA extraction per gram of dry sediment using qPCR (mean ± 1 SE, n = 3). Letters designate significant differences among the interaction of experimental sites and treatments using Tukey's HSD test ($p < 0.05$). Sites include lower (lower-$OM_{sediment}$), intermediate (int-$OM_{sediment}$) and higher (higher-$OM_{sediment}$) sediment organic matter concentrations.

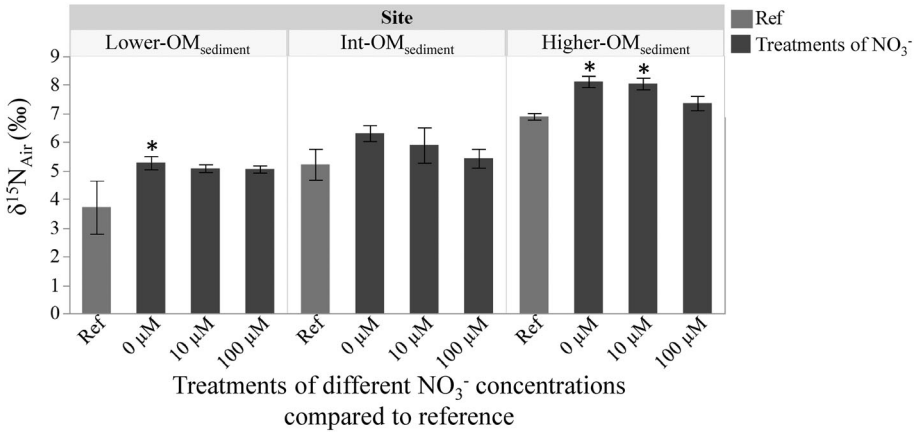

Fig 7. $\delta^{15}N_{Air}$ values of total nitrogen in the top 4 cm layer of incubated sediments compared to the ambient sediments as references collected in the field in the respective experimental site (mean ± 1 SE, n = 3). The asterisk indicated a significant difference between the reference and the incubated sediments from a certain treatment in each site using ANOVA followed by Dunnett's test at $p < 0.05$. Sites include lower (lower-$OM_{sediment}$), intermediate (int-$OM_{sediment}$) and higher (higher-$OM_{sediment}$) sediment organic matter concentrations.

Table 4. Comparison of sediment N_2 fixation and denitrification rates measured under different environmental conditions in estuarine and coastal ecosystems.

Location	Method	Temp* °C	Salinity*	NO_3^- conc.* μM	Organic carbon %	C:N ratio	N_2 fixation μmol N m^{-2} h^{-1}	Denitrification μmol N m^{-2} h^{-1}	*NifH* abundance Copies g^{-1}	References
Yangtze Estuary, China	Slurry incubations with N-isotope tracing	5–30	0–14	221–468†	4.9–17.9	5.9–8.3	23–464	722–4028	2×10^6 to 1×10^8	Hou et al. (2018)
Waquoit Bay, Massachusetts	Flow-through core incubations with N-isotope tracing	18–22	27–32	4‡	NA	8.6	49–103	0–28	5×10^4 to 1×10^5	Newell et al. (2016*b*)
Waquoit Bay, Massachusetts	Batch core incubations with N_2/Ar technique	19–26	27–32	0.1–0.5‡	1.0–6.1	8.6–10.3	12–20	16–64	NA	Foster and Fulweiler (2014)
Narragansett Bay, Rhode Island	Batch core incubations with N_2/Ar technique	17–23	32	NA	NA	NA	0–650	0–530	NA	Fulweiler et al. (2007)
Little lagoon, Alabama	Slurry incubations with acetylene reduction	13–32	23–33	500†	NA	NA	2–3	27–30	4×10^7 to 7×10^7	Bernard et al. (2014, 2015)
Weeks Bay, Alabama	Slurry incubations with acetylene reduction	5–35	0–24	0–55†	NA	NA	8–125	5–72	NA	Mortazavi et al. (2012)
Texas coast, Texas	Flow-through core incubations with N-isotope tracing	11–30	0–38	0–100‡	NA	NA	0–97	0–90	NA	Gardner et al. (2006)
Lake Waco Wetland, Texas	Flow-through core incubations with N-isotope tracing	7–31	0	40–100‡	NA	NA	0–426	54–615	NA	Scott et al. (2008)
Hypoxic zone, Gulf of Mexico	Flow-through core incubations with N-isotope tracing	16–28	34–37	0.6–61‡	0.5–1.8	5.9–8.7	0–147	18–562	NA	McCarthy et al. (2015)
Wax Lake Delta, Louisiana	Flow-through core incubations with N-isotope tracing	20–22	0	0–86‡	0.5–5.5	9.7–11.6	0–437	141–377	1×10^8 to 3×10^9	This study

NA, No data available.
*Parameters measured during incubations.
†Measured in water extracted from sediment (after NO_3^- enrichment).
‡Measured in overlying water column (after NO_3^- enrichment).

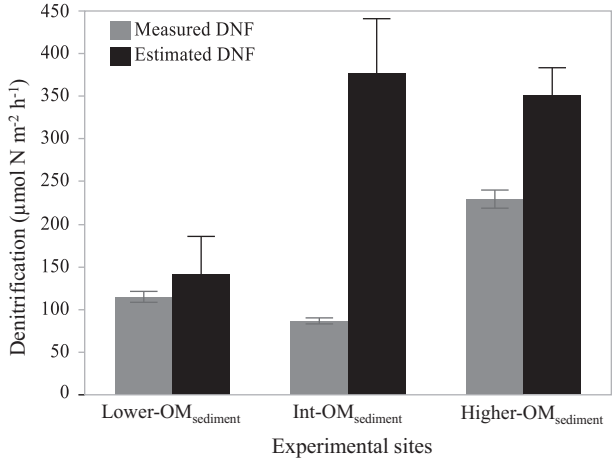

Fig 8. Comparison of denitrification rates measured directly using isotope pairing technique at the 100 μM addition (Li and Twilley, 2021) with estimated denitrification rates using stochiometric assumptions in this study under similar incubation conditions at the same experimental sites.

Delta as a suntropical freshwater ecosystem has lower sulfate concentration that facilitates the growth of diazotrophic bacteria and leads to higher capacity in heterotrophic N_2 fixation (Marino et al. 2003; Howarth and Marino 2006). Our research indicates that N_2 fixation rates were comparable to or exceed denitrification rates under certain environmental conditions, which is also observed in other coastal ecosystems. The change of environmental factors like temperature, salinity, NO_3^- loading and the stoichiometry of carbon, N, and phosphorus leads to a wide range of N_2 fixation rates in different ecosystems (Hou et al. 2018). Methodology difference and extreme events like hurricanes may also cause variations of sediment N_2 fixation and denitrification in different coastal ecosystems (McCarthy et al. 2015). The coastal deltaic floodplain of Wax Lake Delta shows higher capacity in both N_2 fixation as a N source and denitrification as N loss, highlighting the importance of benthic N cycling to water quality conditions before river waters are exported to coastal ocean.

Heterotrophic N_2 fixation rates were lower at higher overlying NO_3^- concentration (100 μM) compared to rates at lower and intermediate NO_3^- concentrations (0 and 10 μM) in each experimental site, which supports the research result that increasing N loading repressed N_2 fixation in wetland sediments (Scott et al. 2008; Moseman-Valtierra et al. 2010). Current NO_3^- concentrations within the Mississippi River Basin vary from 54 to 106 μM, which are around 10 times greater than historical NO_3^- concentrations during the pre-industrial periods in the earlier 20th century (Goolsby et al. 2000; Rabalais et al. 2002; Broussard and Turner 2009). The increased importance of N_2 fixation rates with decreased overlying NO_3^- concentrations especially in the int- and higher-$OM_{sediment}$ sites demonstrated that the net flux of N_2 in the int- and higher-$OM_{sediment}$ sites was likely to be controlled by N_2 fixation as an important source of reactive N when overlying NO_3^- concentration was 10 μM or even lower in the early 1900s (Goolsby et al. 2000). Currently higher NO_3^- concentrations around 100 μM suppresses N_2 fixation, but the inhibited N_2 fixation still equals to 28–50% of total reactive N loss via denitrification when $OM_{sediment}$ concentrations are higher than 6.5% (int- and higher-$OM_{sediment}$ sites). Thus, we propose that a positive net N_2 flux across sediment–water interface at higher NO_3^- concentrations does not preclude the possible occurrence of N_2 fixation. Heterotrophic N_2 fixation, though decreasing with increasing NO_3^- loading, is not totally suppressed under higher NO_3^- concentrations (100 μM). Thus, net N_2 fixation rates estimated from the net uptake of N_2 flux may underestimate the significance of N_2 fixation as N_2 fixation can occur even under higher NO_3^- concentrations.

The int- and higher-$OM_{sediment}$ sites had higher potential in N_2 fixation than the lower-$OM_{sediment}$ site under certain NO_3^- concentration from 0 to 100 μM (Fig. 5). Such variation of N_2 fixation as higher rates occurred with higher $OM_{sediment}$ was reported in other aquatic sediments (Howarth et al. 1988; McCarthy et al. 2016). The increased abundance of *nifH* gene from lower-$OM_{sediment}$ to higher-$OM_{sediment}$ sites also supported the finding that the site with higher $OM_{sediment}$ had higher potential of N_2 fixation than the lower-$OM_{sediment}$ site. It is reasonable that the site with lower $OM_{sediment}$ had lower N_2 fixation and *nifH* abundance as labile organic carbon is an important carbon source for heterotrophic diazotrophs to produce nitrogenase enzyme and fix N (Romero et al. 2012; Fan 2013; McCarthy et al. 2016). Even though the *nifH* gene was present in the lower-$OM_{sediment}$ site, N_2 fixation rates were low in this site. This situation is possible as the presence of *nifH* gene does not necessarily mirror N_2 fixation rates (Zehr et al. 2001; Piehler et al. 2002; Bentzon-Tilia et al. 2015). The abundance of *nifH* gene only indicates the potential capacity of the experimental site to fix N_2 but not represent the actual amount of *nifH* gene expressed under in situ conditions during experimental incubations (Howarth and Marino 2006; Bentzon-Tilia et al. 2015).

It is noteworthy that the absence of N_2 fixation and significantly lower abundance of *nifH* gene in the lower-$OM_{sediment}$ site might be related to the occurrence of Hurricane Barry (McCarthy et al. 2015). Hurricanes can cause substantial mineral sedimentation to the delta, which changes the initial bulk density and $OM_{sediment}$ concentrations (McCarthy et al. 2015; Bevington et al. 2017). However, the bulk density (1.2 g cm^{-3}) and $OM_{sediment}$ concentration (4.5%) in the lower-$OM_{sediment}$ site measured after the hurricane in 2019 were not significantly different with the bulk density (1.5 g cm^{-3}) and $OM_{sediment}$ (2.9%) measured in summer 2018 (Li and Twilley, 2021). The hurricane event induced a sudden increase of surface water salinity from 0.2 to 4.3 within 11 h (data from CRMS 0464 station on the east side of the delta) then dropped back to 0.2 by the date we sampled this area. Our estimated denitrification rates of 141 $\pm$ 44.3 μmol N m^{-2} h^{-1} (100 μM overlying NO_3^-) after Hurricane Barry in summer 2019 are

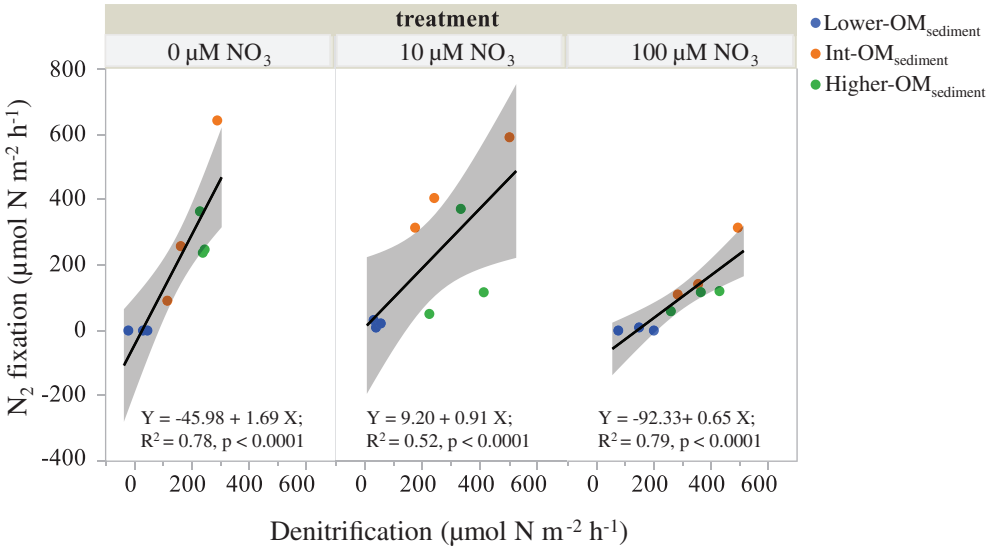

Fig 9. Heterotrophic N_2 fixation rates relative to denitrification rates among the three sites at lower (lower-$OM_{sediment}$), intermediate (int-$OM_{sediment}$), and higher (higher-$OM_{sediment}$) sediment organic matter concentrations in each treatment of NO_3^- addition. F ratio and p values from ANOVA test were shown below each equation.

similar to denitrification rates of 197 ± 17 μmol N m^{-2} h^{-1} measured in summer 2017 (Li et al. 2020) and 115 ± 6.4 μmol N m^{-2} h^{-1} measured in summer 2018 (Li and Twilley, 2021) under similar incubation conditions, indicating benthic denitrification was not significantly impacted by the hurricane event. The lower-$OM_{sediment}$ site is a subtidal site with lower sediment surface elevation (– 0.61 m NAVD88) and is inundated year round (Li et al. 2020). Submersed aquatic vegetation and benthic microalgae dominate the earlier successional zones of delta development in this area. We speculate that the site with lower soil surface elevation had minor benthic disturbance from Hurricane Barry and is representative of lower-$OM_{sediment}$ treatment as used in this study. The absence of N_2 fixation and significantly lower abundance of *nifH* gene in the lower-$OM_{sediment}$ site is very likely to due to lower $OM_{sediment}$ concentrations in this site rather than the hurricane effects. We propose that more field research is necessary before drawing any sound conclusion about hurricane effects on N_2 fixation in the lower-$OM_{sediment}$ site.

Denitrification and its correlation with N_2 fixation

Denitrification rates measured directly with 100 μM $^{15}NO_3^-$ enrichment using isotope pairing technique varied from 87 to 229 μmol N m^{-2} h^{-1} along the increasing gradient of $OM_{sediment}$ in the delta in summer 2018 (Fig. 8, Li and Twilley, 2021). Estimated denitrification rates based on the stochiometric ratio of benthic fluxes (summer 2019) ranged from 141 to 377 μmol N m^{-2} h^{-1} under the similar incubation condition in this research. The estimated denitrification rates are within the same range of the measured denitrification rates, especially in the lower- and higher-$OM_{sediment}$ sites, supporting that the estimate denitrification rates are representative for the real denitrification potential in the three experimental sites. It is noteworthy that certain amount of heterogeneity between estimated and measured denitrification existed as the two studies were conducted at different years.

The significantly higher denitrification rates estimated here in the int- and higher-$OM_{sediment}$ sites compared to the lower-$OM_{sediment}$ site are consistent to the increasing trend of $\delta^{15}N_{Air}$ values in the ambient sediments from the lower-$OM_{sediment}$ to higher-$OM_{sediment}$ sites (light gray columns in Fig. 7). The natural abundance of ^{15}N in ambient sediments reflects a long-term isotopic fractionation with a preferential consumption of lighter ^{14}N and residual of ^{15}N during denitrification, anammox, and/or volatilization (Robinson 2001; Reis et al. 2019). For experimental sites with the same N source, sites with higher denitrification rates usually had higher $\delta^{15}N_{Air}$ values in total N content as more ^{14}N was released from sediments back to atmosphere through denitrification (Bryantmason et al. 2013; Reis et al. 2019). As such, our result of $\delta^{15}N_{Air}$ values increasing from the lower-$OM_{sediment}$ to higher-$OM_{sediment}$ sites in the ambient sediment samples demonstrates that the area with higher $OM_{sediment}$ concentrations had greater N loss to the atmosphere, which supports the finding that higher $OM_{sediment}$ facilitates denitrification in coastal deltaic floodplains (Li et al. 2020; Li and Twilley, 2021).

Heterotrophic N_2 fixation was positively correlated with denitrification in each NO_3^- treatment (Fig. 9) probably because that the increased $OM_{sediment}$ provided favorable conditions for both N_2 fixation and denitrification (Howarth et al. 1988; Henry and Twilley 2014; Li et al. 2020). Greater $OM_{sediment}$ can increase benthic metabolism and expand an anaerobic zone, which then enhance benthic denitrification (Cornwell et al. 1999; Boynton et al. 2018). On the other

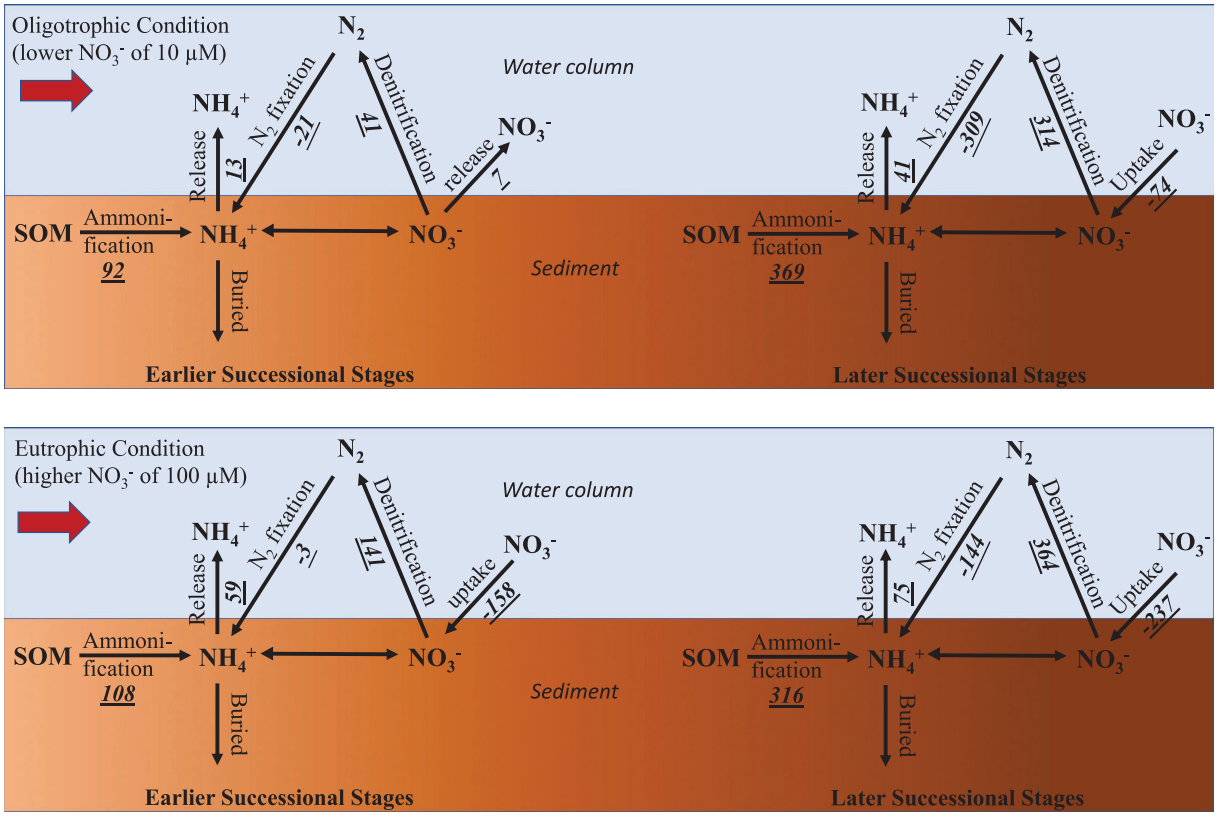

Fig 10. Nitrogen budgets at the sediment–water interface under (**a**) oligotrophic condition with historically lower NO_3^- concentration (10 μM) and (**b**) eutrophic condition with currently higher NO_3^- concentration (100 μM) in study areas representing different successional stages of coastal deltaic floodplain development. The earlier successional stage has lower sediment organic matter concentrations (based on results from the lower-$OM_{sediment}$ site) and the later successional stage has relatively higher sediment organic matter concentrations (based on results from the int- and higher-$OM_{sediment}$ sites). Summarized rates for all four stages of ecosystem development are presented in μmol N m^{-2} h^{-1}. Negative values indicate uptake from overlying water column to deltaic sediments. Ammonification rates were evaluated based on sediment oxygen consumptions divided by the stochiometric ratio of O: NH_4^+ (13.25) in each experimental site (Cowan et al. 1996).

hand, higher $OM_{sediment}$ provided a greater source of labile organic carbon for heterotrophic diazotrophs to generate nitrogenase enzyme for N_2 fixation (Romero et al. 2012; Fan 2013; McCarthy et al. 2016). The slope of the fitted equation was 1.7 when overlying NO_3^- concentration was 0 μM, indicating that N_2 fixation generally outcompeted denitrification under oligotrophic (low NO_3^-concentration) conditions especially when $OM_{sediment}$ concentrations were no < 6.5%. The slope of fitted equation decreased to 0.9 when overlying NO_3^- concentration increased to 10 μM, which means sediment N_2 fixation was barely sufficient to offset N loss via benthic denitrification. However, when the overlying NO_3^- concentration increased to 100 μM, the slope of the fitted equation decreased to 0.7 and the intercept became more negative (–92.3), demonstrating that N_2 fixation was less significant to N loss via denitrification in the eutrophic system. In summary, though N_2 fixation and denitrification both increased with increasing $OM_{sediment}$ concentration, the relative importance of these two processes were impacted mostly by overlying NO_3^- concentrations as increasing NO_3^- gradually switched the dominance of N_2 fluxes from N_2 fixation to denitrification in a coastal deltaic floodplain.

Nitrogen budgets in the emerging coastal deltaic floodplain

We evaluated benthic N budgets with a major focus on N_2 fixation and denitrification under lower and higher overlying NO_3^- concentrations at the earlier and later successional stages of coastal deltaic floodplain development. Benthic fluxes at the earlier successional stage of the delta were based on the results measured from the lower-$OM_{sediment}$ site, whereas benthic fluxes at the later successional stage were based on the averaged results from the int- and higher-$OM_{sediment}$ sites. NH_4^+ production from ammonification was calculated from sediment oxygen consumptions divided by the stochiometric ratio of O: NH_4^+ (13.25) in each experimental site (Cowan et al. 1996). Under historically lower NO_3^- concentration (10 μM), ammonification rates increased from 92 to 369 μmol N m^{-2} h^{-1} in study areas from earlier to later

successional stages, which were higher than respective NH_4^+ release rates from sediments to overlying water columns (13–41 μmol N m^{-2} h^{-1}; Fig. 10a). The difference in NH_4^+ fluxes between ammonification and sediment release to overlying water might represent N buried in wetland sediments and/or converted to NO_3^- via nitrification. Heterotrophic N_2 fixation occurred under both successional stages of delta development but the later successional stage with higher $OM_{sediment}$ concentrations had higher N_2 fixation capacity (309 μmol N m^{-2} h^{-1}) than the earlier successional stage with lower $OM_{sediment}$ concentrations (21 μmol N m^{-2} h^{-1}). Denitrification varied from 41 to 314 μmol N m^{-2} h^{-1} along the increased $OM_{sediment}$ gradient from earlier to later successional stages, but net NO_3^- uptake rates from overlying water to deltaic sediments were no larger than 74 μmol N m^{-2} h^{-1}, indicating that <24% of the removed N via denitrification was from overlying NO_3^- loading directly. Instead, the majority of N removed via denitrification might be from fixed N through heterotrophic N_2 fixation and/or $OM_{sediment}$ ammonification under historically lower overlying NO_3^- concentration.

Under currently higher NO_3^- concentration (100 μM) due to anthropogenic fertilization, ammonification rates were similar to the respective rates at lower overlying NO_3^- concentration (Fig. 10b). NH_4^+ fluxes across sediment–water interface slightly increased compared to the rates at lower NO_3^- loading but were still smaller than the respective ammonification rates. Heterotrophic N_2 fixation rates were inhibited at both successional stages with lower and higher $OM_{sediment}$ concentrations (3 and 144 μmol N m^{-2} h^{-1}, respectively) compared to the corresponding rates under historically lower overlying NO_3^- concentration. However, denitrification rates were facilitated under higher overlying NO_3^- concentration, resulting in an increased significance of denitrification compared to N_2 fixation in dominating benthic N fluxes in coastal deltaic floodplain. Net NO_3^- uptake rates from overlying water to deltaic sediments increased to 158 μmol N m^{-2} h^{-1} at the earlier successional stage and 237 μmol N m^{-2} h^{-1} at the later successional stage due to the increased overlying NO_3^- concentration. The comparable rates between denitrification and benthic NO_3^- uptake under higher overlying NO_3^- concentration demonstrate that deltaic sediments were an important sink of riverine NO_3^- as over 65% of the removed N via denitrification was from riverine NO_3^- loading directly.

Balancing the N budgets in the emerging coastal deltaic floodplain can serve as an analog of benthic N dynamics during different stages of deltaic development in continental margins of major rivers around the world. The evaluation of N budgets at different $OM_{sediment}$ concentrations representing different stages of deltaic development helps to clarify the change of N_2 fixation and denitrification with ecological succession associated with $OM_{sediment}$ accumulations. Comparison of N budgets between historically lower and currently higher NO_3^- loadings advances our understanding of how benthic N dynamics of N_2 fixation and denitrification have been altered by significant increase in riverine NO_3^- due to anthropogenic fertilization. However, benthic N dynamics were more complex than analyzed here since other sources of N like groundwater input, atmospheric deposition, and autotrophic N_2 fixation may also play an important role in N input in natural ecosystems (Nixon et al. 1995). Also, except for N_2 fixation and denitrification evaluated in this research, other co-occurred N pathways like coupled nitrification–denitrification and dissimilatory nitrate reduction to ammonium (DNRA) and the possible occurrence of anammox may alter benthic N dynamics in coastal deltaic floodplains (Li and Twilley, 2021). Further analysis of model simulation that accounts for all the possible N input and output as well as natural hydrodynamic conditions may provide a more clear and accurate evaluation of benthic N budget in coastal deltaic floodplains in continental margins of major rivers.

Conclusion

We evaluated heterotrophic N_2 fixation rates in a newly emergent coastal deltaic floodplain in Mississippi River Delta using continuous flow-through incubations with $^{30}N_2$ enrichment. The occurrence of heterotrophic N_2 fixation was supported by the presence of *nifH* gene and the increased $\delta^{15}N$ of total N in sediment cores after incubation. The results indicated that increasing NO_3^- loading decreased N_2 fixation rates and increased denitrification rates at each $OM_{sediment}$ concentration in wetland sediments. However, the decreased N_2 fixation rates under higher NO_3^- concentration (100 μM) still equal to 28–50% of N loss via denitrification, demonstrating the importance of N_2 fixation as a N source in benthic N cycling. Both N_2 fixation and denitrification increased with $OM_{sediment}$ concentrations, but the relative importance of these two processes was impacted mostly by overlying NO_3^- concentrations as increasing NO_3^- gradually switched a dominance of N_2 fixation to a dominance of denitrification in benthic N cycling in a coastal deltaic floodplain. The evaluation of benthic N budgets focusing on N_2 fixation and denitrification reveals that N_2 fixation was comparable to denitrification under historically lower NO_3^- concentrations (10 μM). The majority removed N (≥76%) via denitrification at historically lower NO_3^- concentrations was from heterotrophic N_2 fixation and/or $OM_{sediment}$ ammonification rather than riverine NO_3^- loading. In contrast, currently higher overlying NO_3^- concentration (100 μM) makes denitrification the dominant benthic N pathway compared to N_2 fixation and over 65% of the removed N via denitrification was from riverine NO_3^- loading. This study highlights the importance of N_2 fixation and clarifies the variation mechanism of N_2 fixation and denitrification in a newly emergent coastal delta in response to increased NO_3^- loading. We propose that the quantification of heterotrophic N_2 fixation is necessary to evaluate coastal N budget not only in oligotrophic environment but also in eutrophic environment.

References

An, S., W. S. Gardner, T. Kana, and K. Universitetsbibliotek. 2001. Simultaneous measurement of denitrification and nitrogen fixation using isotope pairing with membrane inlet mass spectrometry analysis simultaneous measurement of denitrification and nitrogen fixation using isotope pairing with membrane inlet mass spectro. Appl. Environ. Microbiol. **67**: 1171–1178.doi:10.1128/AEM.67.3.1171

Bentzon-Tilia, M., S. J. Traving, M. Mantikci, H. Knudsen-Leerbeck, J. L. S. Hansen, S. Markager, and L. Riemann. 2015. Significant N_2 fixation by heterotrophs, photoheterotrophs and heterocystous cyanobacteria in two temperate estuaries. ISME J. **9**: 273–285.doi:10.1038/ismej.2014.119

Bernard, R. J., B. Mortazavi, L. Wang, A. C. Ortmann, H. MacIntyre, and W. C. Burnett 2014. Benthic nutrient fluxes and limited denitrification in a sub-tropical groundwater-influenced coastal lagoon. Marine Ecology Progress Series **504**: 13–26. doi:10.3354/meps10783

Bernard, R. J., B. Mortazavi, and A. A. Kleinhuizen 2015. Dissimilatory nitrate reduction to ammonium (DNRA) seasonally dominates NO3 – reduction pathways in an anthropogenically impacted sub-tropical coastal lagoon. Biogeochemistry **125**: 47–64. doi:10.1007/s10533-015-0111-6

Bevington, A. E., R. R. Twilley, C. E. Sasser, and G. O. Holm 2017. Contribution of river floods, hurricanes, and cold fronts to elevation change in a deltaic floodplain, northern Gulf of Mexico, USA. Estuarine, Coastal and Shelf Science **191**: 188–200. doi:10.1016/j.ecss.2017.04.010

Bevington, A. E., and R. R. Twilley. 2018. Island edge morphodynamics along a chronosequence in a prograding Deltaic Floodplain Wetland. J. Coast. Res. **344**: 806–817. doi:10.2112/jcoastres-d-17-00074.1

Boynton, W. R., M. A. C. Ceballos, E. M. Bailey, C. L. S. Hodgkins, J. L. Humphrey, and J. M. Testa. 2018. Oxygen and nutrient exchanges at the sediment-water interface: A global synthesis and critique of estuarine and coastal data. Estuaries Coast **1**: 301–333.

Broussard, W., and R. E. Turner. 2009. A century of changing land-use and water-quality relationships in the continental US. Front. Ecol. Environ. **7**: 302–307.doi:10.1890/080085

Bryantmason, A., Y. J. Xu, and M. Altabet. 2013. Isotopic signature of nitrate in river waters of the lower Mississippi and its distributary, the Atchafalaya. Hydrol. Process. **27**: 2840–2850.doi:10.1002/hyp.9420

Canfield, D. E., A. N. Glazer, and P. G. Falkowski. 2010. The evolution and future of earth's nitrogen cycle. Science **330**: 192–196.doi:10.1126/science.1186120

Capone, D., D. Bronk, M. Mulholland, and E. Carpenter. 2008. Nitrogen in the marine environment. Elsevier.

Cornwell, J. C., W. M. Kemp, and T. M. Kana. 1999. Denitrification in coastal ecosystems: Methods, environmental controls, and ecosystem level controls, a review. Aquat Ecol **33**: 41–54.

Cowan, J. L. W., J. R. Pennock, and W. R. Boynton. 1996. Seasonal and interannual patterns of sediment-water nutrient and oxygen fluxes in Mobile Bay, Alabama (USA): regulating factors and ecological significance. Marine Ecology Progress Series **141**: 229–245. doi:10.3354/meps141229

Damashek, J., and C. A. Francis. 2018. Microbial nitrogen cycling in estuaries: From genes to ecosystem processes. Estuar. Coast. **41**: 626–660.doi:10.1007/s12237-017-0306-2

Delwiche, C. C. 1970. The nitrogen cycle. Sci. Am. **223**: 136–146.doi:10.1038/scientificamerican0970-136

Dias, A. C. F., M. C. Pereira e Silva, S. R. Cotta, and others. 2012. Abundance and genetic diversity of nifH gene sequences in anthropogenically affected Brazilian Mangrove sediments. Appl. Environ. Microbiol. **78**: 7960–7967. doi:10.1128/AEM.02273-12

Edmonds, D. A., C. Paola, D. C. J. D. Hoyal, and B. A. Sheets. 2011. Quantitative metrics that describe river deltas and their channel networks. J. Geophys. Res. Earth **116**: 1–15. doi:10.1029/2010JF001955

Eyre, B. D., S. S. Rysgaard, T. Dalsgaard, and P. B. Christensen. 2002. Comparison of isotope pairing and N2:Ar methods for measuring sediment denitrification: Assumptions, modifications, and implications. Estuaries **25**: 1077–1087.doi:10.1007/BF02692205

Fan, L. 2013. Response of diazotrophic microbial community to nitrogen input and glyphosate application in soils cropped to soybean. Auburn University.

Foster, S. Q., and R. W. Fulweiler. 2014. Spatial and historic variability of benthic nitrogen cycling in an anthropogenically impacted estuary. Frontiers in Marine Science **1**: 1–16. doi:10.3389/fmars.2014.00056

de Felippes, F. F., and D. Weigel. 2010. Chapter 17 transient assays for the analysis of miRNA processing and function. Plant microRNA Methods **592**: 255–264.doi:10.1007/978-1-60327-005-2

Fulweiler, R. W., S. W. Nixon, B. A. Buckley, and S. L. Granger. 2007. Reversal of the net dinitrogen gas flux in coastal marine sediments. Nature **448**: 180–182.doi:10.1038/nature05963

Fulweiler, R. W., S. M. Brown, S. W. Nixon, and B. D. Jenkins. 2013. Evidence and a conceptual model for the co-occurrence of nitrogen fixation and denitrification in heterotrophic marine sediments. Mar. Ecol. Prog. Ser. **482**: 57–68.doi:10.3354/meps10240

Galloway, J. N., W. H. Schlesinger, H. Levy, A. Michaels, and J. L. Schnoor. 1995. Nitrogen fixation: Anthropogenic enhancement-environmental response. Global Biogeochem Cycles **9**: 235–252.doi:10.1029/95GB00158

Gardner, W. S., M. J. McCarthy, S. An, D. Sobolev, K. S. Sell, and D. Brock. 2006. Nitrogen fixation and dissimilatory nitrate reduction to ammonium (DNRA) support nitrogen

dynamics in Texas estuaries. Limnol. Oceanogr. **51**: 558–568.doi:10.4319/lo.2006.51.1_part_2.0558

Goolsby, D. A., W. A. Battaglin, B. T. Aulenbach, and R. P. Hooper. 2000. Nitrogen flux and sources in the Mississippi River basin. Sci. Total Environ. **248**: 75–86.doi:10.1016/S0048-9697(99)00532-X

Henry, K. M., and R. R. Twilley. 2014. Nutrient biogeochemistry during the early stages of delta development in the Mississippi River deltaic plain. Ecosystems **17**: 327–343.doi:10.1007/s10021-013-9727-3

Herbert, R. A. 1999. Nitrogen cycling in coastal marine ecosystems. FEMS Microbiol. Rev. **23**: 563–590.doi:10.1016/S0168-6445(99)00022-4

Hiatt, M., and P. Passalacqua. 2015. Hydrological connectivity in river deltas: The first-order importance of channel-Island exchange. Water Resour. Res. **51**: 2264–2282.doi:10.1002/2014WR016149

Hoffman, D. K., M. J. McCarthy, S. E. Newell, W. S. Gardner, D. N. Niewinski, J. Gao, and T. R. Mutchler. 2019. Relative contributions of DNRA and denitrification to nitrate reduction in *Thalassia testudinum* seagrass beds in coastal Florida (USA). Estuar. Coast **42**: 1001–1014.doi:10.1007/s12237-019-00540-2

Hou, L., R. Wang, G. Yin, M. Liu, and Y. Zheng. 2018. Nitrogen fixation in the intertidal sediments of the Yangtze estuary: Occurrence and environmental implications. J. Geophys. Res. Biogeosci. **123**: 936–944.doi:10.1002/2018JG004418

Howarth, R. W., R. Marino, J. Lane, and J. J. Cole. 1988. Nitrogen fixation in freshwater, estuarine, and marine ecosystems. 1. Rates and importance. Limnol. Oceanogr. **33**: 669–687.doi:10.4319/lo.1988.33.4part2.0669

Howarth, R. W., and R. Marino. 2006. Nitrogen as the limiting nutrient for eutrophication in coastal marine ecosystems: Evolving views over three decades. Limnol. Oceanogr. **51**: 364–376.

Kana, T. M., C. Darkangelo, M. D. Hunt, J. B. Oldham, G. E. Bennett, and J. C. Cornwell. 1994. Membrane lnlet mass spectrometer for rapid environmental water samples. Anal. Chem. **66**: 4166–4170.

Klotz, M. G., and L. Y. Stein. 2008. Nitrifier genomics and evolution of the nitrogen cycle. FEMS Microbiol. Lett. **278**: 146–156.doi:10.1111/j.1574-6968.2007.00970.x

Knapp, A. N. 2012. The sensitivity of marine N2 fixation to dissolved inorganic nitrogen. Front. Microbiol. **3**: 1–14.doi:10.3389/fmicb.2012.00374

Koop-Jakobsen, K., and A. E. Giblin. 2010. The effect of increased nitrate loading on nitrate reduction via denitrification and DNRA in salt marsh sediments. Limnol. Oceanogr. **55**: 789–802.doi:10.4319/lo.2009.55.2.0789

Lane, R. R., J. W. Day, B. Marx, E. Reyes, and G. P. Kemp. 2002. Seasonal and spatial water quality changes in the outflow plume of the Atchafalaya River, Louisiana, USA. Estuaries **25**: 30–42.doi:10.1007/BF02696047

Li, S., A. Christensen, and R. R. Twilley. 2020. Benthic fluxes of dissolved oxygen and nutrients across hydrogeomorphic zones in a coastal deltaic floodplain within the Mississippi River Delta plain. Biogeochemistry **149**: 115–140.

Li, S., and R. R. Twilley. 2021. Nitrogen dynamics of inundated sediments in an emerging coastal deltaic floodplain in mississippi river delta using isotope pairing technique to test response to nitrate enrichment and sediment organic matter. Estuaries and Coasts. doi:10.1007/s12237-021-00913-6

Marino, R., R. W. Howarth, F. Chan, J. J. Cole, and G. E. Likens. 2003. Sulfate inhibition of molybdenum-dependent nitrogen fixation by planktonic cyanobacteria under seawater conditions: A non-reversible effect. Hydrobiologia **500**: 277–293.doi:10.1023/A:1024641904568

McCarthy, M. J., S. E. Newell, S. A. Carini, and W. S. Gardner. 2015. Denitrification dominates sediment nitrogen removal and is enhanced by bottom-water hypoxia in the Northern Gulf of Mexico. Estuar. Coast **38**: 2279–2294.doi:10.1007/s12237-015-9964-0

McCarthy, M. J., W. S. Gardner, M. F. Lehmann, A. Guindon, and D. F. Bird. 2016. Benthic nitrogen regeneration, fixation, and denitrification in a temperate, eutrophic lake: Effects on the nitrogen budget and cyanobacteria blooms. Limnol. Oceanogr. **61**: 1406–1423.doi:10.1002/lno.10306

Miller-Way, T., and R. R. Twilley. 1996. Theory and operation of continuous flow systems for the study of benthic-pelagic coupling. Mar. Ecol. Prog. Ser. **140**: 257–269.doi:10.3354/meps140257

Mortazavi, B., A. A. Riggs, J. M. Caffrey, H. Genet, and S. W. Phipps. 2012. The contribution of benthic nutrient regeneration to primary production in a shallow eutrophic estuary, weeks bay, alabama. Estuaries and Coasts **35**: 862–877. doi:10.1007/s12237-012-9478-y

Moseman-Valtierra, S. M., K. Armaiz-Nolla, and L. A. Levin. 2010. Wetland response to sedimentation and nitrogen loading: Diversification and inhibition of nitrogen-fixing microbes. Ecol. Appl. **20**: 1556–1568.doi:10.1890/08-1881.1

Mulholland, M. R., K. Ohki, and D. G. Capone. 2001. Nutrient controls on nitrogen uptake and metabolism by natural populations and cultures of Trichodesmium (Cyanobacteria). J. Phycol. **37**: 1001–1009.doi:10.1046/j.1529-8817.2001.00080.x

Newell, S. E., M. J. McCarthy, W. S. Gardner, and R. W. Fulweiler. 2016*a*. Sediment nitrogen fixation: A call for re-evaluating coastal N budgets. Estuar. Coast **39**: 1626–1638. doi:10.1007/s12237-016-0116-y

Newell, S. E., K. R. Pritchard, S. Q. Foster, and R. W. Fulweiler. 2016*b*. Molecular evidence for sediment nitrogen fixation in a temperate New England estuary. PeerJ **2016**: 1–21.doi:10.7717/peerj.1615

Nielsen, L. P., and R. N. Glud. 1996. Denitrification in a coastal sediment measured in situ by the nitrogen isotope

pairing technique applied to a benthic flux chamber. Mar. Ecol. Prog. Ser. **137**: 181–186.doi:10.3354/meps137181

Nixon, S. W., S. L. Granger, and B. L. Nowicki. 1995. An assessment of the annual mass balance of carbon, nitrogen, and phosphorus in Narragansett Bay. Biogeochemistry **31**: 15–61. doi:10.1007/bf00000805

Paola, C., R. R. Twilley, D. A. Edmonds, W. Kim, D. Mohrig, G. Parker, E. Viparelli, and V. R. Voller. 2011. Natural processes in delta restoration: Application to the Mississippi delta. Ann. Rev. Mar. Sci. **3**: 67–91.doi:10.1146/annurev-marine-120709-142856

Piehler, M. F., J. Dyble, P. H. Moisander, J. L. Pinckney, and H. W. Paerl. 2002. Effects of modified nutrient concentrations and ratios on the structure and function of the native phytoplankton community in the Neuse River estuary, North Carolina, USA. Aquat Ecol **36**: 371–385.doi:10.1023/A:1016529015349

Poly, F., L. J. Monrozier, and R. Bally. 2001. Improvement in the RFLP procedure for studying the diversity of nifH genes in communities of nitrogen fixers in soil. Res. Microbiol. **152**: 95–103.doi:10.1016/S0923-2508(00)01172-4

Postgate, J. R. 1970. Biological nitrogen fixation. Nature **226**: 25–27.doi:10.1038/226025a0

Rabalais, N. N., R. E. Turner, Q. Dortch, D. Justic, V. J. Bierman, and W. J. Wiseman. 2002. Nutrient-enhanced productivity in the northern Gulf of Mexico: Past, present and future. Hydrobiologia **475–476**: 39–63.doi:10.1023/A:1020388503274

Reis, C. R. G., S. C. Reed, R. S. Oliveira, and G. B. Nardoto. 2019. Isotopic evidence that nitrogen enrichment intensifies nitrog
en losses to the atmosphere from subtropical mangroves. Ecosystems **22**: 1126–1144.doi:10.1007/s10021-018-0327-0

Robinson, D. 2001. δ15N as an integrator of the nitrogen cycle. Trends Ecol. Evol. **16**: 153–162.doi:10.1016/S0169-5347(00)02098-X

Romero, I. C., M. Jacobson, J. A. Fuhrman, M. Fogel, and D. G. Capone. 2012. Long-term nitrogen and phosphorus fertilization effects on N_2 fixation rates and nifH gene community patterns in mangrove sediments. Mar. Ecol. **33**: 117–127.doi:10.1111/j.1439-0485.2011.00465.x

Scott, J. T., M. J. McCarthy, W. S. Gardner, and R. D. Doyle. 2008. Denitrification, dissimilatory nitrate reduction to ammonium, and nitrogen fixation along a nitrate concentration gradient in a created freshwater wetland. Biogeochemistry **87**: 99–111. doi:10.1007/s10533-007-9171-6

Twilley, R. R., and others. 2019. Ecogeomorphology of coastal deltaic floodplains and estuaries in an active delta: Insights from the Atchafalaya Coastal Basin. Estuarine, Coastal and Shelf Science **227**: 106341. doi:10.1016/j.ecss.2019.106341

Vitousek, P. M., J. D. Aber, R. W. Howarth, G. E. Likens, P. A. Matson, D. W. Schindler, W. H. Schlesinger, and D. G. Tilman. 1997. Human alteration of the global nitrogen cycle: Sources and consequences. Ecol. Appl. **7**: 737–750. doi:10.1890/1051-0761(1997)007[0737:HAOTGN]2.0.CO;2

Welsh, D. T. 2000. Nitrogen fixation in seagrass meadows: Regulation, plant-bacteria interactions and significance to primary productivity. Ecol. Lett. **3**: 58–71.doi:10.1046/j.1461-0248.2000.00111.x

Welsh, D. T., S. Bourguès, R. De Wit, and I. Auby. 1997. Effect of plant photosynthesis, carbon sources and ammonium availability on nitrogen fixation rates in the rhizosphere of *Zostera noltii*. Aquat. Microb. Ecol. **12**: 285–290.doi:10.3354/ame012285

Zehr, J. P., J. B. Waterbury, P. J. Turner, J. P. Montoya, E. Omoregie, G. F. Steward, A. Hansen, and D. M. Karl. 2001. Unicellular cyanobacteria fix N2 in the subtropical North Pacific Ocean. Nature **412**: 635–638.doi:10.1038/35088063

Zehr, J. P., B. D. Jenkins, S. M. Short, and G. F. Steward. 2003. Nitrogenase gene diversity and microbial community structure: A cross-system comparison. Environ. Microbiol. **5**: 539–554.doi:10.1046/j.1462-2920.2003.00451.x

Acknowledgments

This study was supported by the National Science Foundation via the Coastal SEES program at LSU [EAR-1427389]. This manuscript was prepared under award R/MMR-33 to Louisiana Sea Grant College Program by NOAA's Office of Ocean and Atmospheric Research, U.S. Department of Commerce. We would like to thank Jiusheng Ren, Silvia E. Newell, Thomas Blanchard, and Alexandra Christensen for analytical support and field support.

Conflict of Interest

None declared.

Submitted 06 May 2020
Revised 26 October 2020
Accepted 15 January 2021

Associate editor: Ronnie N. Glud